

Micro Fresnel Zone Plate Lens Inscribed on a Hard Polymer Clad Fiber Using Femtosecond Pulsed Laser

Jongki Kim, Woosung Ha, Jiyoung Park, Jun Ki Kim, Ik-Bu Sohn, Woojin Shin, and Kyunghwan Oh

Abstract—We report a novel process to directly inscribe a Fresnel zone plate (FZP) lens on the cleaved facet of a hard clad polymer fiber using a femtosecond pulsed laser. The FZPs are designed by adopting modal analysis and free-space diffraction, which are experimentally implemented by locally ablating silica glass using femtosecond laser pulses. A good agreement between the design and fabricated FZP lens is obtained with an exceptionally long focal length over 600 m, which can have a strong potential in all-fiber beam shaping technology and optical interconnections.

Index Terms—Beam shaping, Fresnel zone plate, laser ablation, lensed fiber.

I. INTRODUCTION

MULTIMODE fiber (MMF) components with a large core area have been developed for various optical applications. One of them is the optical interconnection in optical printed circuit board (PCB), short reach (SR) or very short reach (VSR) optical communications [1]. As the focusing capability in MMF devices became a critical property in these applications, recent commercial packages have been developed with a separate micro-lens mounted on a holder, which is, however, inherently vulnerable to external vibrations and suffers from a rather tight tolerance in the alignment. To overcome these shortcomings, integration of micro-lens on the fiber ends has been intensively studied in recent years [2]–[4]. The authors have developed an all-fiber solution to embed polymer micro-lens on the cleaved facet of hard polymer clad fiber (HPCF) for connecting arrays of vertical cavity surface emitting laser (VCSEL) [5]. In comparison to conventional refractive lenses, Fresnel zone plates (FZPs) utilizes the

diffraction and interference nature of the coherent electromagnetic wave to achieve a focusing capability in a compact flat plane [6]. This plane FZP has been highly appreciated in various imaging and non-imaging applications to remove or alleviate the tight demand for the curvature radius control in the refractive lenses. Furthermore FZPs have reduced optical design burdens in both scaling-up and scaling down. The authors have made a preliminary attempt to inscribe micro FZP over a serially concatenated single mode fiber (SMF)/coreless silica fiber (CSF) using femtosecond laser processing [7]. CSF was introduced to expand the beam from the SMF core, and this scheme required meticulous CSF length control in the μm length scale and careful optimization for SMF/CSF splice, which significantly hindered mass fabrication for practical uses. Despite increasing demands for integration of MMF and focusing optics in the optical interconnection applications, the possibility to combine FZP in MMF, especially HPCF, have not been fully explored yet. In this letter, we proposed a new hybrid integrated all-fiber device, FZP inscribed on the end-facet of HPCF. Theoretically, we investigated the device's unique beam focusing capability by combining the mode analyses in the HPCF and subsequently their free-space diffraction through the FZP. Experimentally we employed a highly precise femto-second laser ablation process to directly write FZPs over the cleaved end-facet of HPCF, for the first time. The focusing properties of the integrated FZP over HPCF were investigated and we found a good agreement between the theoretical design and experimental measurement.

II. EXPERIMENTS AND RESULTS

Ultra-short pulse lasers have been intensively developed in recent years for various material processing applications. Among them, the femtosecond pulsed laser has shown significant potential in ultra-high precision with significantly reduced process debris, as well as flexible control of depth and area [8]. We employed an amplified femtosecond pulsed Ti: Sapphire laser system to pattern the FZP on the silica glass core of HPCF. The experimental schematic is illustrated in Fig. 1(a). The laser was operated at $\lambda = 785.5$ nm in a pulsed mode with the repetition rate of 1 kHz and the pulse duration of 184 fs. The pulse energy was measured to be about $0.45 \mu\text{J}$. The laser output passed through a shutter and reflected on a dichroic mirror. The reflected laser beam was focused by an objective lens with 50-times magnification and 0.42 numerical aperture (NA). Detailed beam parameters were described elsewhere [7]. The HPCF had the core diameter of $200 \mu\text{m}$, which is composed of pure silica glass surrounded by a low refractive

Manuscript received May 4, 2012; revised January 2, 2013; accepted February 16, 2013. Date of publication March 7, 2013; date of current version March 29, 2013. This work was supported in part by the Brain Korea 21 Project, in part by the NRF of Korea and a grant funded by the Korea government (MEST) (2011-00181613, 2012M3A7B4049800), and in part by the Seoul R&BD Program (PA110081).

J. Kim, J. Park, and K. Oh are with the Department of Physics, Yonsei University, Seoul 120-749, Korea (e-mail: kim.jongki@yonsei.ac.kr; jy_park@yonsei.ac.kr; koh@yonsei.ac.kr).

W. Ha is with the Department of Physics, Yonsei University, Seoul 120-749, Korea, and also with the Research Engineer/3D Group, LG Electronics, Seoul 137-724, Korea (e-mail: wha@yonsei.ac.kr).

J. K. Kim is with the Department of Physics, Yonsei University, Seoul 120-749, Korea, and also with the Wellman Center for Photomedicine, Harvard Medical School, Boston, MA 02114 USA (e-mail: satsix@naver.com).

I.-B. Sohn and W. Shin are with the Advanced Photonics Research Institute (APRI), Gwangju 500-712, Korea (e-mail: ibson@gist.ac.kr; swj6290@gist.ac.kr).

Color versions of one or more of the figures in this letter are available online at <http://ieeexplore.ieee.org>.

Digital Object Identifier 10.1109/LPT.2013.2249506

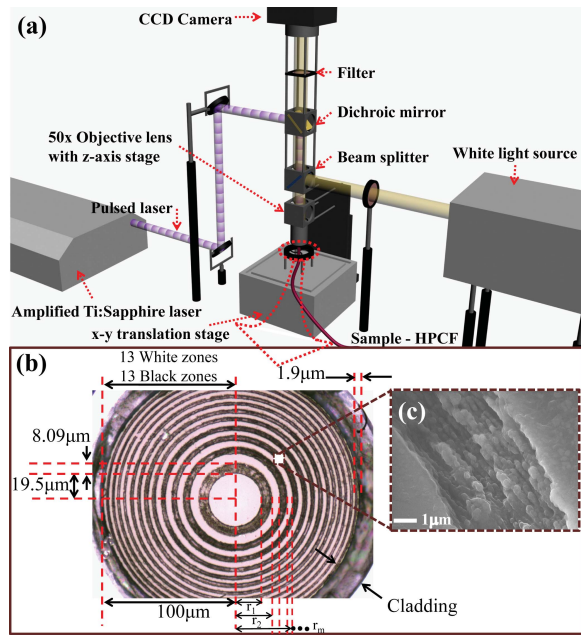


Fig. 1. (a) Schematic diagram of the device fabrication setup. (b) Cross-sectional image of the fabricated FZP directly inscribed on HPCF. (c) SEM image of the laser-ablated surface.

index polymer cladding. A high optical quality facet end of HPCF was prepared using an ultrasonic fiber cleaver. The prepared HPCF was mounted on a nano-rotation/translation stage and the end-facet was aligned perpendicular to the focused laser beam. The laser beam waist was about $0.5 \mu\text{m}$ and the ablation processing speed was around $5\sim 8 \mu\text{m/s}$. The FZP rings' radii are given as [9], [10]:

$$r_m = \sqrt{m\lambda r_0 + \left(\frac{m\lambda}{2}\right)^2}. \quad (1)$$

Here, r_m is the radius of the m -th circle, r_0 is the focal length of the FZP at the signal light wavelength λ . In this experiment, the signal light was He-Ne laser at $\lambda = 635 \text{ nm}$ and the focal length, r_0 , was $600 \mu\text{m}$.

The fabricated FZP on HPCF end-facet is shown in Fig. 1(b), where the laser processed region, "Black zone," is optically opaque and the pristine region, "White zone," is transparent. Across the end-facet, we inscribed total 13 "White zones," and 13 "Black zones." The central "White zone" had the radius of $19.5 \mu\text{m}$ and the width of the innermost and the outermost "Black zones" were $8.09 \mu\text{m}$ ($= r_2 - r_1$) and $1.9 \mu\text{m}$ ($= r_{13} - r_{12}$), respectively. Detailed surface of the "Black zones" was examined using a scanning electron microscope (SEM) with the electron energy of 15.0 kW and the result is shown in Fig. 1(c). The focused femto-second laser pulses ablated the silica to result in sub-micron embossing with the surface roughness of several hundred nm, which served as an optically opaque region for the incident signal light at $\lambda = 635 \text{ nm}$ by efficient local scattering. In contrast, the pristine surface preserved the high optical flatness providing a high transmission. The total engraving area was $1.56 \times 10^4 \mu\text{m}^2$ which corresponded to 49.7% of the entire core cross-section. Note that the spatial precision of the proposed process is equivalent to conventional E-beam or UV

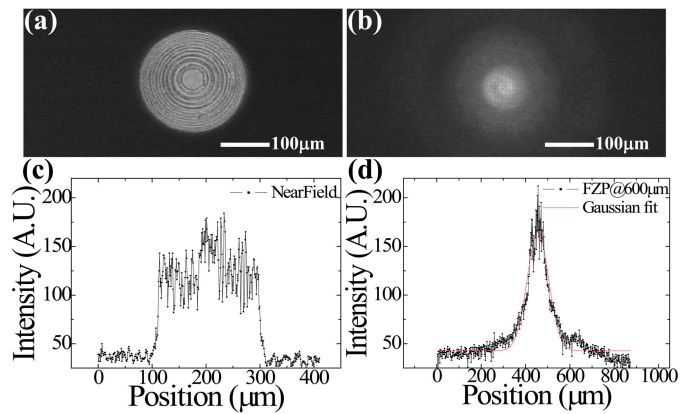


Fig. 2. (a) Experimentally measured near-field image of the output beam from the fabricated device and (b) experimentally measured far-field image, at the axial position $z = 600 \mu\text{m}$ from the fabricated device. Line intensity profiles in (c) near field and (d) far field at $z = 600 \mu\text{m}$ along with a Gaussian curve fitting.

light lithography, yet the total process time, ~ 1 hour, was significantly reduced by the direct inscribing procedures. Note that this process can be further expanded to arrays of HPCF that can provide even higher fabrication throughputs.

Transmission of the a red laser ($\lambda = 635 \text{ nm}$) through the fabricated FZP was experimentally investigated by measuring the beam images and intensity profiles along the axial direction with a charge coupled device (CCD) camera, and the results are summarized in Fig. 2. The near-field image and its line intensity profile are shown in Fig. 2(a) and (c), respectively. Corresponding measurements for the far-field image at the axial position of $600 \mu\text{m}$, the estimated focal length of FZP, are shown in Fig. 2(b) and (d). It is clearly observed that the FZP on HPCF did show an efficient focusing capability such that a near-flat top intensity profile with the diameter of $\sim 200 \mu\text{m}$ at the near field was transformed to a nearly Gaussian beam with the full width at half maximum (FWHM) of $\sim 90 \mu\text{m}$ as shown in Fig. 2(d). It is also noted that the axial position with the minimum FWHM of $\sim 90 \mu\text{m}$ was extended from 550 to $650 \mu\text{m}$, providing an excellent longitudinal alignment tolerance over $100 \mu\text{m}$ as well as a longest focal length obtained in fiber optic lenses.

The focusing capability of the proposed device was theoretically analyzed in two steps: 1) identifying the guided modes in HPCF by using finite element method (FEM) tool, Mode solutionsTM, to define the input optical intensity profile, 2) investigating propagation of the modal intensity profiles through the designed FZP and subsequent diffraction along the free space using a beam propagation solver, Virtual LabTM of LightTrans GmbH. The core of HPCF had the refractive index of silica glass, $n_{\text{core}} = 1.4569$ at $\lambda = 635 \text{ nm}$ with the diameter of $200 \mu\text{m}$. The low refractive index polymer cladding had $n_{\text{clad}} = 1.4400$, and the outer diameter of $230 \mu\text{m}$. The fundamental mode had the effective refractive index n_{eff} of 1.44937 , and the average spacing of n_{eff} between the adjacent higher modes was found to be $\sim 1 \times 10^{-6}$ to result in the total guided mode number of $\sim 10^4$. In order to investigate the beam propagation through the proposed device, we selected 1, 10, 100, and 1,000 guided modes. These modes were coherently added and their transmission through the FZP

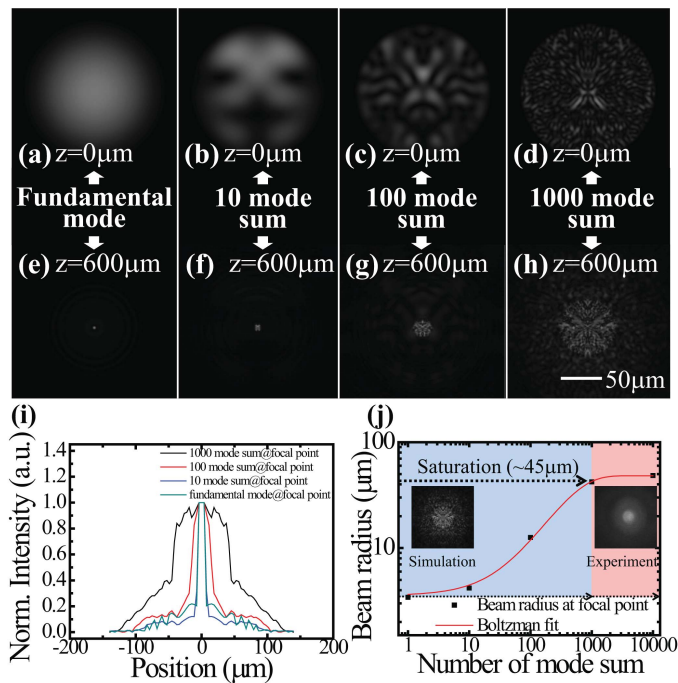


Fig. 3. Theoretical prediction of the near-field intensity profile, $z = 0 \mu\text{m}$, for (a) fundamental mode, (b) ten modes, (c) 100 modes, and (d) 1000 modes guided along the HPCF. Theoretical prediction of intensity profiles at $z = 600 \mu\text{m}$, the focal length of the FZP for (e) fundamental mode, (f) ten modes, (g) 100 modes, (h) 1000 modes. (i) theoretical prediction of the line profile of the beam intensity at the focal plane for various number of modes used in the simulations, and (j) beam waist variation simulation as a function of the number of modes, and comparison with the experimental data.

was calculated using the beam propagation tool. The numerical results for the output beam propagation are summarized in Fig. 3. Here we compared the simulation results of the near-field in the following cases: (a) only the fundamental mode was considered, (b) 10 modes, (c) 100 modes, and (d) 1,000 modes were considered. The corresponding far-field images at the axial position $z = 600 \mu\text{m}$ are shown in (e)~(h). The far-field simulation converged to the experimental measurement in Fig. 2(b) as the number of modes increased to 1,000. It is noted that the FWHM of the beam rapidly increased due to the modal interference, which is summarized in Fig. 3(i). The FWHM of the far-field beam took a converging value of $\sim 90 \mu\text{m}$ as the number of modes increased to 1,000 and beyond as in Fig. 3(j). Note that this theoretical FWHM is very consistent to the experimental value.

After confirming the agreement between the simulation and measurements for the near field and the far field images at $z = 600 \mu\text{m}$, we then further investigated the evolution of the far field pattern along the axial direction from 0 to $800 \mu\text{m}$. The measurements and simulation results are summarized in Fig. 4(a) and (b), respectively. The numerical analysis showed a good agreement with experiments having the focal length of $\sim 600 \mu\text{m}$, despite the fact that we took account only 1000 out of $\sim 10^4$ guided modes. It is also noted that the focused beam out of the proposed device showed a large tolerance in the focal length such that the minimum FWHM beam diameter of $90 \mu\text{m}$ maintained along the axial distance as long as $\sim 100 \mu\text{m}$, which was confirmed in both experiments and simulation as in Fig. 3(i). This unique beaming property would

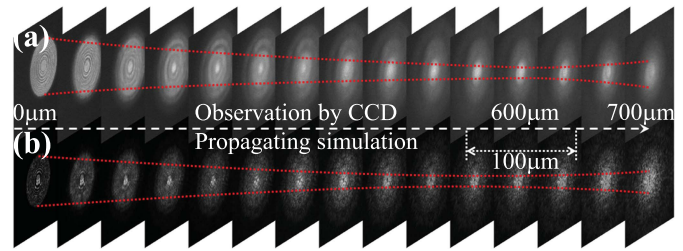


Fig. 4. Comparison between (a) experiments and (b) simulations for the beam propagation through the proposed FZP on HPCF along the axial position.

be of a highly practical value in the optical interconnection to allow a large tolerance in the beam alignments.

III. CONCLUSION

In this study, we experimentally demonstrated direct inscription of FZP using a femto-second laser, over a cleaved end-facet of HPCF that had the silica core diameter of $200 \mu\text{m}$. Sub-micron roughness in the ablated region provided optical opaqueness and total of 26 Fresnel zones were formed with the central zone diameter of $19.5 \mu\text{m}$. In experiments, we obtained the focal length of $\sim 600 \mu\text{m}$ and the minimum beam diameter of $\sim 90 \mu\text{m}$, which were maintained over $100 \mu\text{m}$ in the axial direction providing a unique tolerance in the longitudinal alignment. We numerically analyzed the proposed device using the modal analysis, followed by the beam propagation simulation. We found a good agreement between the measurements and simulations for the focal length, its tolerance, and the beam diameter. From our study, we confirmed a compact beam shaping capability of the proposed FZP on HPCF, and its unique large tolerance in the focal length would have an ample potential for free space optical interconnects among multimode optical fiber based devices and micro-optic beam shaping.

REFERENCES

- [1] D. U. Kim, S. C. Bae, J. Kim, T.-Y. Kim, C.-S. Park, and K. Oh, "Hard polymer cladding fiber (HPCF) links for high-speed short reach 1×4 passive optical network (PON) based on all-HPCF compatible fused taper power splitter," *IEEE Photon. Technol. Lett.*, vol. 17, no. 11, pp. 2355–2357, Nov. 2005.
- [2] K. Shiraishi and S.-I. Kuroo, "A new lensed-fiber configuration employing cascaded GI-fiber chips," *J. Lightw. Technol.*, vol. 18, no. 6, pp. 787–794, Jun. 2000.
- [3] W. J. Tomlinson, "Applications of GRIN-rod lenses in optical fiber communication systems," *Appl. Opt.*, vol. 19, no. 7, pp. 1127–1138, 1980.
- [4] M. Sasaki, T. Ando, S. Nogawa, and K. Hane, "Direct photolithography on optical fiber end," *Jpn. J. Appl. Phys.*, vol. 41, no. 6B, pp. 4350–4355, 2002.
- [5] J. K. Kim, D. U. Kim, B. H. Lee, and K. Oh, "Arrayed multimode fiber to VCSEL coupling for short reach communications using hybrid polymer-fiber lens," *IEEE Photon. Technol. Lett.*, vol. 19, no. 13, pp. 951–953, Jul. 1, 2007.
- [6] W. Watanabe, D. Kuroda, K. Itoh, and J. Nishii, "Fabrication of Fresnel zone plate embedded in silica glass by femtosecond laser pulses," *Opt. Express*, vol. 10, no. 19, pp. 978–983, 2002.
- [7] J. Kim, *et al.*, "Fabrication of micro Fresnel zone plate lens on a mode expanded hybrid optical fiber using a femto-second laser ablation system," *IEEE Photon. Technol. Lett.*, vol. 21, no. 1, pp. 21–23, Jan. 1, 2009.
- [8] B. N. Chichkov, C. Momma, S. Nolte, F. von Alvensleben, and A. Tünnermann, "Femtosecond, picosecond and nanosecond laser ablation of solids," *Appl. Phys. A*, vol. 63, pp. 109–115, 1996.
- [9] A. Michette, "Zone plates," in *Handbook of Optics*, vol. 5, M. Bass Ed. New York, USA: McGraw-Hill, 2010, pp. 40.1–40.11.
- [10] E. Hecht, *Optics*, 4th ed. Reading, MA, USA: Addison-Wesley, 2002, pp. 493–506.